Extended Rank Reduction Estimator for Noncircular Sources

Chong Li[1, a], Xiaowen Li [2, b] and Xiaobao Fu[3, c]

[1]National Digital Switching System Engineering and Technology Research Center, Zhengzhou 450000, China;

[2]Henan Financial Institute, Zhengzhou 450000, China;

[3]Zhengzhou Science and Technology Institute, Zhengzhou 450000, China.

[a]xxgclichong@163.com, [b]13203702095@sohu.com, [c]21845801@qq.com

Abstract. Researchers have placed much attention on direction-of-arrival (DOA) estimation algorithms for noncircular sources in recent years. However, inevitable sensor errors will cause considerable deterioration of estimation performance of these algorithms. This paper proposes an extended rank reduction estimator (RARE, a kind of auto-calibration methods) for noncircular sources upon a condition of factorization of the steering vectors in the presence of sensor errors. The proposed method can realize the “decoupling” estimation of DOAs and sensor errors without any iterative process. The simulation results of two different applications of the proposed method are presented, which demonstrate that the proposed method outperforms the conventional RARE in terms of estimation accuracy and the number of sources that can be distinguished. Moreover, its performance advantage in estimation accuracy is more significant when signal-to-noise ratio is low, or the number of snapshots is small.

Keywords: DOA Estimation, auto-calibration, extended RARE, noncircular Source, identifiability.

1. Introduction

Noncircular signals (e.g., binary-phase-shift-keying (BPSK), multiple-amplitude-shift-keying (MASK), and offset-quadrature-phase-shift-keying (OQPSK) modulated signals) are widely used in modern communication and satellite communication systems, thus increasing researchers have placed attention on direction-of-arrival (DOA) estimation algorithms for noncircular sources [1-3]. The direction-finding methods exploiting noncircular property have higher accuracy of estimation compared with conventional algorithms (e.g., multiple signal classification (MUSIC) algorithm [4] and algorithms based on estimation of signal parameters via rotational invariance techniques (ESPRIT) [5]). However, inevitable sensor errors will lead to considerable deterioration of estimation performance in reality, and those super-resolution estimators that assume the steering vectors are precisely known may even fail the desired performance. Therefore, the study on sensor error calibration technologies is quite significant. Among all the calibration methods, one auto-calibration method—rank reduction estimator (RARE) [6-9] is extensively applied because of its advantages—high estimation accuracy and resolution without any iterative process. At present, there are not adequate RARE methods for noncircular signals, and thus the number of sources that existing methods can distinguish is limited and their estimation accuracy has yet to be improved.

Under this background, this paper focuses on utilizing noncircular property of signals to further improve the auto-calibration performance. Based on the principle of the conventional RARE, i.e., RARE methods without exploiting noncircular property of signals, our method can also achieve “decoupling” estimation (i.e., estimation of DOAs and sensor error parameters in turn without any iterative process). In addition, the special structure of the extended covariance matrix of noncircular signals with maximum noncircularity rate is applied, which can provide much more information than the conventional model regarding circular signals. Two sets of simulations are conducted to calibrate mutual coupling and angularly dependent gain/phase errors.

Copyright © 2019, the Authors. Published by Atlantis Press.
This is an open access article under the CC BY-NC license (http://creativecommons.org/licenses/by-nc/4.0/).

The following notations are used throughout the paper. (1) $[\cdot]^*$, $[\cdot]^{\mathrm{T}}$, $[\cdot]^{\mathrm{H}}$ stand for conjugate, transpose, conjugate transpose, respectively; (2) $\mathrm{diag}[\cdot]$ indicates the composition of diagonal matrix; (3) $\det[\cdot]$ is the determinant; (4) $\mathrm{E}[\cdot]$ is the expectation; (5) $\mathbf{C}^{N\times M}$ and $\mathbf{R}^{N\times M}$ signify the set of $N\times M$ complex matrices and the set of $N\times M$ real matrices, respectively.

2. Data Model

Assuming s to be a noncircular signal with zero-mean, then variance and unconjugated variance of s satisfy the following equation

$$\mathrm{E}[s^2]=\rho e^{\mathrm{j}\phi}\mathrm{E}[|\mathrm{s}|^2] \quad (1)$$

where ρ denotes the noncircularity rate satisfying $0\le\rho\le1$, and ϕ is the noncircularity phase. In this paper, we consider the signal with maximum noncircularity rate (i.e., $\rho=1$), and this case corresponds to BPSK, MASK modulated signals.

The far-field narrowband signal is usually used for DOA estimation. Here, a noisy mixture of N narrow-band sources having DOAs is assumed to impinge on an array composed of M sensors. The N source signals are uncorrelated. The associated observation vector, whose components are the complex envelopes of the signals at the output of the sensors under sensor errors, is thus given by

$$\boldsymbol{x}(t)=\boldsymbol{B}\boldsymbol{s}(t)+\boldsymbol{n}(t) \quad (2)$$

where $\boldsymbol{s}(t)\in\mathbf{C}^{N\times1}$ is the source vector, whose elements are complex envelopes of the signals with maximum noncircularity rate at the input of the sensors, and $\boldsymbol{n}(t)\in\mathbf{C}^{M\times1}$ is the white and complex circular noise vector mixed through the sensors. $\boldsymbol{B}$ is an $M\times N$ matrix containing N corresponding steering vectors in the presence of sensor errors , and is expressed as

$$\boldsymbol{B}=\left[\boldsymbol{b}(\theta_1,\boldsymbol{\eta}_1),\boldsymbol{b}(\theta_2,\boldsymbol{\eta}_2),\cdots\boldsymbol{b}(\theta_N,\boldsymbol{\eta}_N)\right] \quad (3)$$

where subscript n denotes the nth signal source, θ_n represents the DOA parameter and $\boldsymbol{\eta}_n$ is the vector of sensor errors. Specifically, $\boldsymbol{\eta}_n$ is angularly independent when channel gain/phase error or mutual coupling exists, and it becomes angularly dependent when the isotropy of array element is not satisfied or multiple sensor errors exist.

Using the property of noncircularity, the covariance matrix $\boldsymbol{R}_x$ and unconjugated covariance matrix $\boldsymbol{R}'_x$ of the observation $\boldsymbol{x}(t)$ are

$$\boldsymbol{R}_x=\mathrm{E}[\boldsymbol{x}(t)\boldsymbol{x}^{\mathrm{H}}(t)]=\boldsymbol{B}\boldsymbol{R}_s\boldsymbol{B}^{\mathrm{H}}+\sigma_n^2\boldsymbol{I}_M\,; \quad (4)$$

$$\boldsymbol{R}'_x=\mathrm{E}[\boldsymbol{x}(t)\boldsymbol{x}^{\mathrm{T}}(t)]=\boldsymbol{B}\boldsymbol{R}'_s\boldsymbol{B}^{\mathrm{T}} \quad (5)$$

in which σ_n^2 denotes the white noise power, and $\boldsymbol{I}_M$ is an $M\times M$ identity matrix, and $\boldsymbol{R}_s=\mathrm{E}[\boldsymbol{s}(t)\boldsymbol{s}^{\mathrm{H}}(t)]$, $\boldsymbol{R}'_s=\mathrm{E}[\boldsymbol{s}(t)\boldsymbol{s}^{\mathrm{T}}(t)]$. Since the signals are uncorrelated, and with maximum noncircularity rate, the unconjugated covariance matrix $\boldsymbol{R}'_x$ can be expressed as

$$\boldsymbol{R}'_x=\boldsymbol{B}\boldsymbol{\Phi}\boldsymbol{R}_s\boldsymbol{B}^{\mathrm{T}} \quad (6)$$

where $\boldsymbol{\Phi}=\mathrm{diag}[e^{\mathrm{j}\phi_1},e^{\mathrm{j}\phi_2}\cdots e^{\mathrm{j}\phi_N}]$ with ϕ_n being the noncircularity phase of the nth source. For the unconjugated characteristic of noncircularity, we extend $\boldsymbol{x}(t)$ to

$$\boldsymbol{y}(t)=[\boldsymbol{x}^{\mathrm{T}}(t),\boldsymbol{x}^{\mathrm{H}}(t)]^{\mathrm{T}}. \quad (7)$$

Using Eq. 4 and Eq. 6, the diagonal structure of $\boldsymbol{R}_s$ leads to a compressed expression of the covariance matrix of $\boldsymbol{y}(t)$ as following

$$\boldsymbol{R}_y=\mathrm{E}[\boldsymbol{y}(t)\boldsymbol{y}^{\mathrm{H}}(t)]=\boldsymbol{B}_{\mathrm{NC}}\boldsymbol{R}_s\boldsymbol{B}_{\mathrm{NC}}^{\mathrm{H}}+\sigma_n^2\boldsymbol{I}_{2M} \quad (8)$$

where $\boldsymbol{B}_{\mathrm{NC}}=[\boldsymbol{B}^{\mathrm{T}},\boldsymbol{\Phi}^*\boldsymbol{B}^{\mathrm{H}}]^{\mathrm{T}}$ is the extended steering matrix. Hence, the extended steering vector of the nth noncircular source is

$$\boldsymbol{b}_{\mathrm{NC}}(\theta_n,\phi_n,\boldsymbol{\eta}_n)=[\boldsymbol{b}^{\mathrm{T}}(\theta_n,\boldsymbol{\eta}_n),\boldsymbol{b}^{\mathrm{H}}(\theta_n,\boldsymbol{\eta}_n)e^{-\mathrm{j}\phi_n}]^{\mathrm{T}}\,. \tag{9}$$

Different from the steering vector $\boldsymbol{b}(\theta_n,\boldsymbol{\eta}_n)$ based on the circular model, the extended steering vector $\boldsymbol{b}_{\mathrm{NC}}(\theta_n,\phi_n,\boldsymbol{\eta}_n)$ contains not only the information of DOA and sensor errors, but also the information of noncircular phase.

3. Extended RARE

It has been shown in [6] that the criterion of RARE algorithm can be concentrated with respect to DOA, leading to a simpler procedure conditioned on factorization of the steering vector as follows (We are not to explain how to factorize $\boldsymbol{b}(\theta_n,\boldsymbol{\eta}_n)$ since the necessary details have been given in many literatures.)

$$\boldsymbol{b}(\theta_n,\boldsymbol{\eta}_n)=\boldsymbol{T}(\theta_n)\boldsymbol{f}(\boldsymbol{\eta}_n)\qquad n=1,2,\cdots N \tag{10}$$

where $\boldsymbol{T}(\theta_n)$ is a vector function of DOA parameter given by

$$\boldsymbol{T}(\theta_n)=[\boldsymbol{t}_1(\theta_n),\boldsymbol{t}_2(\theta_n)\cdots\boldsymbol{t}_{N_t}(\theta_n)]\in\mathbf{C}^{M\times N_t}\,, \tag{11}$$

and $\boldsymbol{f}(\boldsymbol{\eta}_n)\in\mathbf{C}^{N_t\times 1}$ is a vector function of sensor errors where N_t is the dimension of the sensor error parameters.

When $\boldsymbol{b}(\theta_n,\boldsymbol{\eta}_n)$ can be factorized as expressed in Eq. 10, the extended steering vector $\boldsymbol{b}_{\mathrm{NC}}(\theta_n,\phi_n,\boldsymbol{\eta}_n)$ is also factorized into two parts: one is concerned with only the DOA parameter, while the other is related to the noncircular phase and sensor errors.

Inserting Eq. 10 into Eq. 9, we have

$$\boldsymbol{b}_{\mathrm{NC}}(\theta_n,\phi_n,\boldsymbol{\eta}_n)=[\boldsymbol{f}^{\mathrm{T}}(\boldsymbol{\eta}_n)\boldsymbol{T}^{\mathrm{T}}(\theta_n),\boldsymbol{f}^{\mathrm{H}}(\boldsymbol{\eta}_n)\boldsymbol{T}^{\mathrm{H}}(\theta_n)e^{-\mathrm{j}\phi_n}]^{\mathrm{T}}=\tilde{\boldsymbol{T}}(\theta_n)\boldsymbol{f}'(\boldsymbol{\eta}_n,\phi_n),\ n=1,2\cdots N \tag{12}$$

in which $\tilde{\boldsymbol{T}}(\theta_n)=\mathrm{blkdiag}[\boldsymbol{T}(\theta_n),\boldsymbol{T}^*(\theta_n)]\in\mathbf{C}^{2M\times 2N_t}$ and $\boldsymbol{f}'(\boldsymbol{\eta}_n,\phi_n)=[\boldsymbol{f}^{\mathrm{T}}(\boldsymbol{\eta}_n),\boldsymbol{f}^{\mathrm{H}}(\boldsymbol{\eta}_n)e^{-\mathrm{j}\phi_n}]^{\mathrm{T}}\in\mathbf{C}^{2N_t\times 1}$.

Similar to the conventional RARE, our method is also based on Subspace Orthogonal principle [4], i.e., steering vectors are all orthogonal to noise subspace. Next, we proceed to introduce the orthogonal projector matrix onto the extended noise subspace.

From Eq. 8, the eigenvalues of the extended covariance matrix $\boldsymbol{R}_y$ can be sorted as below [10]

$$\lambda_1\geq\lambda_2\cdots\geq\lambda_N>\lambda_{N+1}=\cdots=\lambda_{2M}=\sigma_n^2\,. \tag{13}$$

Its eigenvectors are divided into two groups: One is signal subspace $\boldsymbol{U}_s\in\mathbf{C}^{2M\times N}$ whose components are eigenvectors $\boldsymbol{e}_1,\boldsymbol{e}_2\cdots,\boldsymbol{e}_N$ corresponding to dominant eigenvalues, and the other is noise subspace $\boldsymbol{U}_n\in\mathbf{C}^{2M\times(2M-N)}$ whose components are eigenvectors $\boldsymbol{e}_{N+1},\boldsymbol{e}_{N+2}\cdots,\boldsymbol{e}_{2M}$ corresponding to small eigenvalue σ_n^2. Therefore, the orthogonal projector matrix onto the extended noise subspace is obtained by

$$\boldsymbol{\Pi}_{\mathrm{NC}}^{\perp}=\boldsymbol{I}_{2M}-\boldsymbol{U}_s\boldsymbol{U}_s^{\mathrm{H}}=\boldsymbol{U}_n\boldsymbol{U}_n^{\mathrm{H}}\in\mathbf{C}^{2M\times 2M} \tag{14}$$

whose dimension is twice as large as the dimension of conventional noise subspace.

In the light of Subspace Orthogonal principle, the following equality holds

$$\boldsymbol{b}_{\mathrm{NC}}^{\mathrm{H}}(\theta_n,\phi_n,\boldsymbol{\eta}_n)\boldsymbol{\Pi}_{\mathrm{NC}}^{\perp}\boldsymbol{b}_{\mathrm{NC}}(\theta_n,\phi_n,\boldsymbol{\eta}_n)=0\qquad n=1,2\cdots N\,. \tag{15}$$

Then putting Eq. 12 into the above equality yields

$$\boldsymbol{f}'^{\mathrm{H}}(\boldsymbol{\eta}_n,\phi_n)\boldsymbol{Q}(\theta_n)\boldsymbol{f}'(\boldsymbol{\eta}_n,\phi_n)=0 \tag{16}$$

with

$$\boldsymbol{Q}(\theta_n)=\tilde{\boldsymbol{T}}^{\mathrm{H}}(\theta_n)\boldsymbol{\Pi}_{\mathrm{NC}}^{\perp}\tilde{\boldsymbol{T}}(\theta_n)\in\mathbf{C}^{2N_t\times 2N_t}\,. \tag{17}$$

For the reason that $\boldsymbol{f}'(\boldsymbol{\eta}_n,\phi_n)\neq\boldsymbol{0}$ and $\boldsymbol{Q}(\theta_n)$ is positive semidefinite, we can infer that the matrix $\boldsymbol{Q}(\theta)$ is full rank unless $\theta=\theta_n\left(n=1,2\cdots N\right)$, i.e., its determinant satisfies

$$D(\theta_n)=\det\left[\boldsymbol{Q}(\theta_n)\right]=0\quad n=1,2\cdots N\,. \tag{18}$$

In practical applications, the orthogonal projector matrix is often estimated by performing the eigenvalue decomposition of the sample covariance $\boldsymbol{R}_{y,L}=\sum_{t=1}^{L}\boldsymbol{y}(t)\boldsymbol{y}^{\mathrm{H}}(t)/L$ based on L numbers of snapshots. Denote the orthogonal projector matrix associated with the noise subspace of $\boldsymbol{R}_{y,L}$ by $\boldsymbol{\Pi}_{\mathrm{NC},L}^{\perp}$. Then following from Eq. 18, the DOA estimators can be obtained by one-dimensional search to minimize

$$D(\theta)=\det[\boldsymbol{Q}_L(\theta)]=\det[\tilde{\boldsymbol{T}}^{\mathrm{H}}(\theta)\boldsymbol{\Pi}_{\mathrm{NC},L}^{\perp}\tilde{\boldsymbol{T}}(\theta)]. \tag{19}$$

Considering that the special structure of $\boldsymbol{\Pi}_{\mathrm{NC},L}^{\perp}$ has been proved in [2], we will present another tractable expression of the objective function $D(\theta)$.

According to [2], $\boldsymbol{\Pi}_{\mathrm{NC},L}^{\perp}$ is structured as

$$\boldsymbol{\Pi}_{\mathrm{NC},L}^{\perp}=\begin{bmatrix}\boldsymbol{\Pi}_{1,L}^{\perp}\ ,\boldsymbol{\Pi}_{2,L}^{\perp}\\ \boldsymbol{\Pi}_{2,L}^{\perp *},\boldsymbol{\Pi}_{1,L}^{\perp *}\end{bmatrix} \tag{20}$$

where $\boldsymbol{\Pi}_{1,L}^{\perp}$ and $\boldsymbol{\Pi}_{2,L}^{\perp}$ are positive semidefinite and complex symmetric, respectively. After substituting the above equality into $\boldsymbol{Q}_L(\theta)=\tilde{\boldsymbol{T}}^{\mathrm{H}}(\theta)\boldsymbol{\Pi}_{\mathrm{NC},L}^{\perp}\tilde{\boldsymbol{T}}(\theta)$, $\boldsymbol{Q}_L(\theta)$ has the structure as

$$\boldsymbol{Q}_L(\theta)=\begin{bmatrix}\boldsymbol{Q}_{11,L}(\theta),\ \boldsymbol{Q}_{12,L}(\theta)\\ \boldsymbol{Q}_{21,L}(\theta),\ \boldsymbol{Q}_{22,L}(\theta)\end{bmatrix} \tag{21}$$

with

$$\begin{cases}\boldsymbol{Q}_{11,L}(\theta)=\boldsymbol{T}^{\mathrm{H}}(\theta)\boldsymbol{\Pi}_{1,L}^{\perp}\boldsymbol{T}(\theta);\ \boldsymbol{Q}_{12,L}(\theta)=\boldsymbol{T}^{\mathrm{H}}(\theta)\boldsymbol{\Pi}_{2,L}^{\perp}\boldsymbol{T}^{*}(\theta);\\ \boldsymbol{Q}_{21,L}(\theta)=\boldsymbol{T}^{\mathrm{T}}(\theta)\boldsymbol{\Pi}_{2,L}^{\perp *}\boldsymbol{T}(\theta);\ \boldsymbol{Q}_{22,L}(\theta)=\boldsymbol{T}^{\mathrm{T}}(\theta)\boldsymbol{\Pi}_{1,L}^{\perp *}\boldsymbol{T}^{*}(\theta).\end{cases} \tag{22}$$

Because $\boldsymbol{\Pi}_{1,L}^{\perp}$ is not a projection matrix [2], the determinant of $\boldsymbol{Q}_{11,L}$ satisfies $\det[\boldsymbol{Q}_{11,L}]\neq 0$ when $\theta=\theta_n(n=1,2\cdots N)$. Then using the readily-checked formula of determinant [11] $\det[\boldsymbol{Q}_L]=\det[\boldsymbol{Q}_{11,L}]\det[\boldsymbol{Q}_{22,L}-\boldsymbol{Q}_{21,L}\boldsymbol{Q}_{11,L}^{-1}\boldsymbol{Q}_{12,L}]$, the estimation of DOA can be computed by minimizing $\det[\boldsymbol{Q}_{22,L}-\boldsymbol{Q}_{21,L}\boldsymbol{Q}_{11,L}^{-1}\boldsymbol{Q}_{12,L}]$.

Thus the following optimization model presents the problem solved for $\hat{\theta}_n$

$$\begin{cases}\hat{\theta}_n=\underset{\theta}{\operatorname{argmin}}\,D(\theta)\qquad n=1,2\cdots N,\\ D(\theta)=\det[\boldsymbol{Q}_{22,L}-\boldsymbol{Q}_{21,L}\boldsymbol{Q}_{11,L}^{-1}\boldsymbol{Q}_{12,L}]=\det[\boldsymbol{T}^{\mathrm{T}}(\theta)\boldsymbol{\pi}_L(\theta)\boldsymbol{T}^{*}(\theta)].\end{cases} \tag{23}$$

where $\boldsymbol{\pi}_L(\theta)=\boldsymbol{\Pi}_{1,L}^{\perp *}-\boldsymbol{\Pi}_{2,L}^{\perp *}\boldsymbol{T}(\theta)\left(\boldsymbol{T}^{\mathrm{H}}(\theta)\boldsymbol{\Pi}_{1,L}^{\perp}\boldsymbol{T}(\theta)\right)^{-1}\boldsymbol{T}^{\mathrm{H}}(\theta)\boldsymbol{\Pi}_{2,L}^{\perp}$. It is remarkable that the estimators minimizing $\det[\boldsymbol{Q}_L]$ and $\det[\boldsymbol{Q}_{22,L}-\boldsymbol{Q}_{21,L}\boldsymbol{Q}_{11,L}^{-1}\boldsymbol{Q}_{12,L}]$ have the same asymptotic distribution and hence they have the same asymptotic performance [4].

Then according to Eq. 16, the estimation of $\boldsymbol{f}'(\boldsymbol{\eta}_n,\phi_n)$ is the eigenvector corresponding to the smallest eigenvalue of $\boldsymbol{Q}_L(\hat{\theta}_n)$. Generally, we can normalize $\boldsymbol{f}'(\boldsymbol{\eta}_n,\phi_n)$ by taking its first element as reference, and hence $\hat{\boldsymbol{f}}'(\hat{\boldsymbol{\eta}}_n,\hat{\phi}_n)$ is solved by

$$\hat{\boldsymbol{f}}'(\hat{\boldsymbol{\eta}}_n,\hat{\phi}_n)=\boldsymbol{e}_{\min}[\boldsymbol{Q}_L(\hat{\theta}_n)]\ \text{with}\ [\boldsymbol{e}_{\min}]_1=1 \tag{24}$$

in which $\boldsymbol{e}_{\min}$ signifies the eigenvector corresponding to the smallest eigenvalue.

Denote $\hat{\boldsymbol{f}}_n'$ as $\hat{\boldsymbol{f}}'(\hat{\boldsymbol{\eta}}_n,\hat{\phi}_n)$ for conciseness, and consequently the noncircular phase and the vector function of sensor errors are estimated by

$$\begin{cases} \hat{\phi}_n = -\arg\left(\dfrac{1}{N_t} \sum_{i=1}^{N_t} [\hat{\boldsymbol{f}}'_n]_{N_t+i} / [\hat{\boldsymbol{f}}'_n]_i \right); \\ \hat{\boldsymbol{f}}(\hat{\boldsymbol{\eta}}_n) = \dfrac{1}{2}\left([\hat{\boldsymbol{f}}'_n]_{1:N_t} + [\hat{\boldsymbol{f}}'^*]_{(N_t+1):2N_t} / [\hat{\boldsymbol{f}}'^*]_{N_t+1} \right). \end{cases} \tag{25}$$

After $\hat{\boldsymbol{f}}(\hat{\boldsymbol{\eta}}_n)$ is got, the estimation of senor errors can be calculated according to the specific structure of $\boldsymbol{f}(\boldsymbol{\eta}_n)$ for different applications.

4. Numerical Results

The purpose of this section is to prove the effectiveness of the extended RARE for noncircular sources in the presence of sensor errors. Simulations of two different applications of the proposed method are carried out based on 500 independent trials. Since RARE can decouple the estimation of DOAs and sensor error parameters, we focus on the DOA estimate errors.

4.1 Extended RARE for Mutual Coupling.

In the first set of experiments, a uniform circular array (UCA) comprising $M = 9$ sensors is employed with its radius $r_{\mathrm{UCA}} = 0.7\lambda$ (λ denotes wavelength). The coupling coefficients are 1, 0.22-0.18j, -0.15+0.16j. Here we make comparisons between the proposed method and the conventional RARE [12] in the presence of mutual coupling.

Two equipowered BPSK modulated sources are assumed with arrival angles given by $\theta_1 = 100^o$ and $\theta_2 = 120^o$. Their noncircularity phases are $\phi_1 = \pi/3\mathrm{rad}$, $\phi_2 = \pi/8\mathrm{rad}$, respectively. Firstly based on $L = 500$ numbers of snapshots, Fig. 1 exhibits the comparison results for two sources against signal to noise ratio (SNR) with its value increasing. Then we simulate the estimation performance with the number of snapshots L ranging from 100 to 1000 when SNR is 5dB. The relevant results for two sources are shown in Fig. 2. We see from these four figures (shown in Fig. 1 and Fig. 2) that the extended RARE outperforms the conventional RARE in terms of RMS errors, and this advantage is more prominent at low SNR values or small number of snapshots.

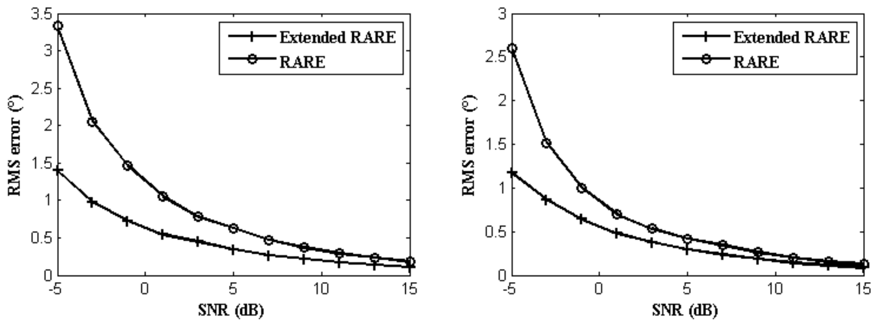

Fig. 1 RMS errors of DOAs for 2 sources versus SNR in the presence of mutual coupling

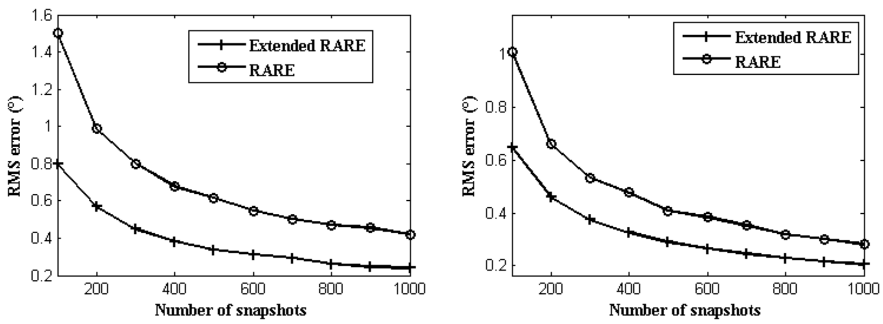

Fig. 2 RMS errors of DOAs for 2 sources versus the number of snapshots in the presence of mutual coupling

4.2 Extended RARE for Angularly Dependent Gain/ Phase Errors.

The second set of experiments is conducted upon the application of a uniform linear array (ULA) with 6 primary sensors in the presence of angularly dependent gain/ phase errors. The adjacent sensor spacing is 0.5λ. The gain errors and phase errors of primary sensors are drawn from the interval [0.5, 2] and the interval [-80°, 80°], respectively. In this section, the estimation results of the proposed method and the conventional instrumental sensor method (ISM—an expansion of RARE) [13,14] will be given. Afterwards, Table 1 lists the numbers of noncircular sources that two methods can handle given different numbers of instrumental sensors (i.e., well-calibrated sensors in advance). The table below illustrates that our proposed method has greater capacity of dealing with unknown parameters compared with the conventional ISM.

Table 1 Numbers of Noncircular Sources That Can Be Estimated with Different Instrumental Sensors in the Presence of Angularly Dependent Gain/ Phase Errors

Numbers of Instrumental Sensors	Methods	
	Extended RARE	Conventional ISM
2	3	1
3	5	2
4	7	3
5	9	4

Then assume that there are three instrumental sensors, and two equipowered BPSK modulated sources with $\phi_1 = \pi/3\text{rad}, \phi_2 = \pi/4\text{rad}$ are from the directions $\theta_1 = 45^o$, $\theta_2 = 75^o$. We also compare the DOA estimation performance of two methods against SNR with its value increasing based on $L = 500$ numbers of snapshots, as depicted in Fig. 3. The same conclusion can be drawn as from Fig. 1. We continue to study the effect of the noncircularity phase separation ($\Delta\phi = |\phi_1 - \phi_2|$) and DOA separation ($\Delta\theta = |\theta_1 - \theta_2|$) on the estimation performance of our method. The relevant results for two sources at SNR=5dB are displayed in Fig.4. It can be seen that the estimate errors of the conventional ISM decreases as $\Delta\theta$ becomes larger, while the estimate errors of the extended RARE are influenced by both $\Delta\theta$ and $\Delta\phi$. Furthermore, our proposed method still performs better than the conventional ISM.

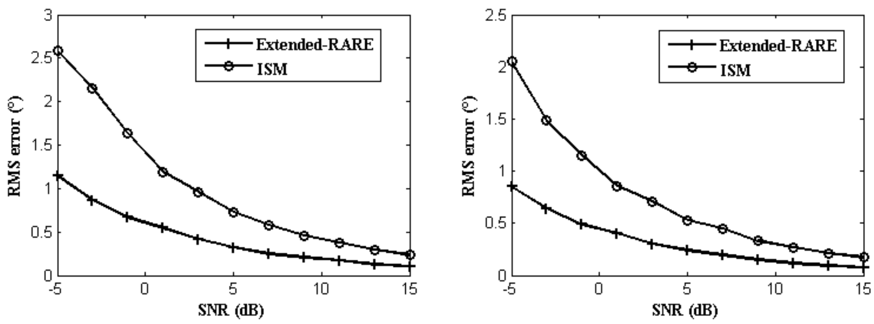

Fig. 3 RMS errors of DOAs for 2 sources versus SNR in the presence of angularly dependent gain/ phase errors

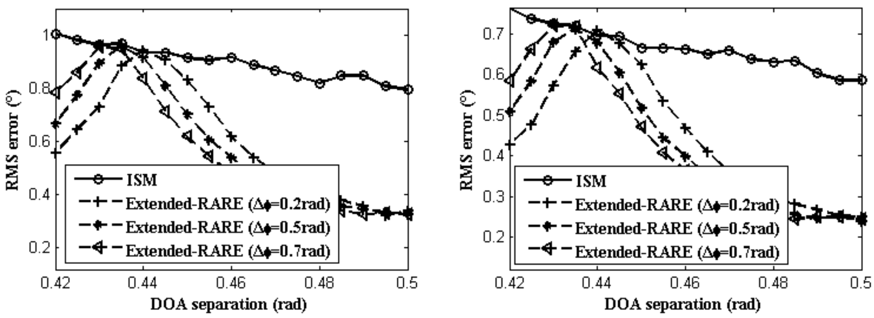

Fig. 4 RMS errors of DOAs for 2 sources versus DOA separation with different noncircularity phase separations in the presence of angularly dependent gain/ phase errors

5. Summary

This paper has presented an extended RARE method for noncircular sources with maximum noncircularity rate in the presence of sensor errors, when the disturbed steering vector has the specified factorization. We have tested the auto-calibration effectiveness of this method upon simulations of two applications. The simulation results illustrate that the proposed method has higher accuracy of estimation and greater capacity of dealing with unknown parameters compared with conventional RARE methods.

References

[1]. Chargé P., Wang Y., Saillard J, "A noncircular sources direction finding method using polynomial rooting," Signal Processing, vol.81, no.6, pp. 1765-1770, 2001.

[2]. Abeida H., Delmas J.-P., "MUSIC-like estimation of direction of arrival for noncircular sources," IEEE Transactions on Signal Processing, vol.54, no.7, pp. 2678-2690, 2006.

[3]. Hassen S. B., Bellili F., Samet A., "DOA estimation of temporally and spatially correlated narrowband noncircular sources in spatially correlated white noise," IEEE Transactions on Signal Processing, vol.59, no.9, pp. 4108-4121, 2011.

[4]. Stoica P., Nehorai A., "MUSIC, Maximum Likelihood, and Cramer-Rao Bound," IEEE Transaction on Acoustics. Speech. & Signal Processing, vol.37, no. 5, pp. 720-741, 1989.

[5]. Roy R., Kailath T., "ESPRIT-estimation of signal parameters via rotational invariance techniques," IEEE Transactions on Acoustics Speech & Signal Processing, vol.37, no. 7, pp. 984-995, 1989.

[6]. Ferréol A., Boyer E., Larzabal P., "Low-cost algorithm for some bearing estimation methods in presence of separable nuisance parameters," Electronics Letters, vol. 40, no. 15, pp. 966-967, 2004.

[7]. Yin J. X., Wu Y., Wang D., "On 2-D direction-of-arrival estimation performance for rank reduction estimator in presence of unexpected modeling errors," Circuits Systems & Signal Processing, vol. 33, no. 2, pp. 515-547, 2014.

[8]. Liu C., Ye Z. F., Zhang Y. F., "Auto-calibration algorithm for mutual coupling of planar array," Signal Processing, vol. 90, no. 3, pp. 784-794, 2010.

[9]. Liang J. L., Zeng X. J., Wang W. Y., Chen H. Y., "L-shaped array-based elevation and azimuth direction finding in the presence of mutual coupling," Signal Processing, vol. 91, no. 5, pp. 1319-1328, 2011.

[10]. Stoica P., Nehorai A., “MUSIC, maximum likelihood, and Cramer-Rao bound: further results and comparisons,” IEEE Transactions on Acoustics Speech & Signal Processing, vol. 38, no. 12, pp. 2140-2150, 1990.

[11]. Zhang X. D., Matrix Analysis and Application. Tsinghua University Press, 2004. (in Chinese)

[12]. Xie J., He Z. S., Li H. Y., “A fast DOA estimation algorithm for uniform circular arrays in the presence of unknown mutual coupling,” Progress in Electromagnetics Research C, vol.21, 2011.

[13]. Wang B. H., Wang Y. L., Chen H., Guo Y., “Array calibration of angularly dependent gain and phase uncertainties with carry-on instrumental sensors,” Science in China Ser.F Information Sciences, vol.34 no.8, pp. 906-918, 2004. (in Chinese)

[14]. Wang B. H., Wang Y. L., Chen H., “Array calibration of angularly dependent gain/phase uncertainties with instrumental sensors,” IEEE International Symposium on Phased Array Systems and Technology, pp. 182-186, 2003.